Cortical excitability controls the strength of mental imagery

Rebecca Keogh†*[1], Johanna Bergmann*[,1,2,3] & Joel Pearson[1]

***shared first authorship**

[1]School of Psychology, University of New South Wales, 2052 Sydney, Australia.

[2]Department of Neurophysiology, Max Planck Institute for Brain Research, Deutschordenstr. 46, 60528 Frankfurt am Main, Germany.

[3]Brain Imaging Center Frankfurt, Goethe-University Frankfurt, Schleusenweg 2-16, 60528 Frankfurt am Main, Germany.

† who correspondence should be directed to: rebeccalkeogh@gmail.com

Abstract

Mental imagery provides an essential simulation tool for remembering the past and planning the future, and its strength affects both cognition and mental health. Research suggests that neural activity spanning prefrontal, parietal, temporal, and visual areas supports the generation of mental images. However, exactly how this network controls the strength of visual imagery remains unknown. Here, brain imaging and transcranial magnetic phosphene data show that lower resting activity and excitability levels in visual cortex (V1-V3), but higher levels in prefrontal cortex, predict stronger sensory imagery. Unlike visual perception, electrically decreasing visual cortex excitability increases imagery strength, while the inverse pattern emerged for prefrontal cortex. These data suggest a neurophysiological mechanism of network cortical excitability that controls the strength of mental images.

Visual imagery is ubiquitous in daily life, and the ability to imagine varies substantially from one individual to another. Due to its highly personal nature, the study of visual imagery has historically relied on self-reported measures and had long been relegated to the shadows of scientific inquiry. However, with the advent of fMRI, its new analysis techniques like decoding, and new advances in behavioral and psychophysical experiments, this is quickly changing (Pearson, 2014). Despite these advances, very little research has investigated why such large individual differences in the ability to imagine exist. Much of the past research focused on the similarities between visual imagery and perception (Kosslyn et al., 1997, Ishai and Sagi, 1995, Pearson et al., 2008), and has shown that a large network of occipital, parietal, and frontal areas are involved when imagining (Pearson et al., 2015). Here, we used a multi-method approach to look at the potential contributions of resting levels of cortical excitability in the visual imagery network as a critical physiological precondition, which determines the strength of visual imagery.

To assess the strength of mental imagery, we utilized the binocular rivalry imagery paradigm, which has been shown to reliably measure the sensory strength of mental imagery through its impact on subsequent binocular rivalry perception. Previous work has demonstrated that when individuals imagine a pattern or are shown a weak perceptual version of a pattern, they are more likely to see that pattern in a subsequent brief binocular rivalry display (Pearson et al., 2015) for review of methods). Longer periods of imagery generation, or weak perceptual presentation, increase the probability of perceptual priming of subsequent rivalry. For this reason, the degree of imagery priming has been taken as a measure of the sensory strength of mental imagery. Importantly, this measure of imagery is directly sensory, and while it is related to subjective reports of imagery vividness, it is not a proxy for metacognitive reports of imagery vividness. This measure of imagery strength has been shown to be both retinotopic location- and spatial orientation-specific (Bergmann et al., 2015, Pearson et al., 2008), is closely related to phenomenal vividness (see supplementary figure S1 and (Pearson et al., 2011), is reliable when assessed over days or weeks (see supplementary figure S2A and (Bergmann et al., 2014), is contingent on the imagery generation period (therefore not due to any rivalry

control) and can be dissociated from visual attention (Pearson et al., 2008). This measure of imagery is advantageous in that it allows us to avoid the prior limitations of subjective introspections and reports, which can often be unreliable and swayed by the context and an individual's ability to introspect (recently referred to as metacognition). Additionally, metacognition appears to be dissociable from the imagery itself, with training-based improvements in imagery metacognition occurring without changes in imagery strength (Rademaker and Pearson, 2012).

Results

Correlations between visual cortex excitability and visual imagery strength

For a first assessment of the relationship between cortex physiology and imagery strength, we looked at fMRI data we collected in a sample of 31 participants during resting-state. We related this data set to each individual's imagery strength determined using the binocular rivalry method (% primed, see Fig.1A). Using a whole-brain surface-based group analysis (see Methods), we found that the mean fMRI intensity of clusters in the visual cortex showed a negative relationship with imagery strength, while frontal cortex clusters showed positive relationships (multiple comparison-corrected; see Fig. S3 and S4 and Supplementary Table S1 and S2).

To further investigate these relationships, we first focused on the visual cortex. We mapped the specific early visual areas V1, V2 and V3 (estimated with standard fMRI retinotopic mapping; see Methods) and the adjacent occipito-parietal areas (defined by the Desikan–Killiany atlas). The extracted estimates of fMRI mean intensity of these ROIs were then normalized by subtracting the whole brain's mean intensity from each ROI's mean intensity, and then dividing it by the whole brain's mean intensity's standard deviation. Following this, we related the normalized mean fMRI intensity scores to each participant's imagery strength; four ROIs showed a significant negative relationship with imagery

strength (V1: r= -.45, p = .01; V2: r= -.45, p = .01; V3 r= -.45, p = .01; lateral occipital area, r= -.49, p < .01: Fig.1D-G).

Despite prior work demonstrating that the binocular rivalry measure of imagery is specific to prior imagery generation and not attentional control of the subsequent rivalry presentation, we performed a control experiment utilizing the known perturbative effect of bright background luminance on imagery generation (Pearson et al., 2008, Keogh and Pearson, 2011, Keogh and Pearson, 2014). Twenty-two of the same participants performed the same imagery task again, however this time with uniform and passive background luminance during the seven second imagery generation. In the presence of background luminance, imagery strength did not significantly correlate with the normalized mean fMRI intensity measure for any visual area (V1: r = -.18, p = .41, V2: r = -.32, p = .15, V3: r = -.40, p = .07, lateral occipital cortex: r = -.34, p = .12). For V1 and V2 these correlations were significantly smaller than their corresponding 'no-luminance' correlations (one-sided Hotelling's t-tests, V1: t(19) = -2.01, p = .029, V2: t(19) = -1.94, p = .034), however the difference in the correlations for V3 and lateral occipital area were not (V3: t(19) = -1.68, p = .055, lateral occipital area t(19)=-1.03, p = .158). As the luminance never co-occurred with the rivalry presentation, it should only interfere with the generation of the images and not the attentional or volitional control of rivalry, suggesting the physiology-behavior relationship cannot be explained by rivalry control.

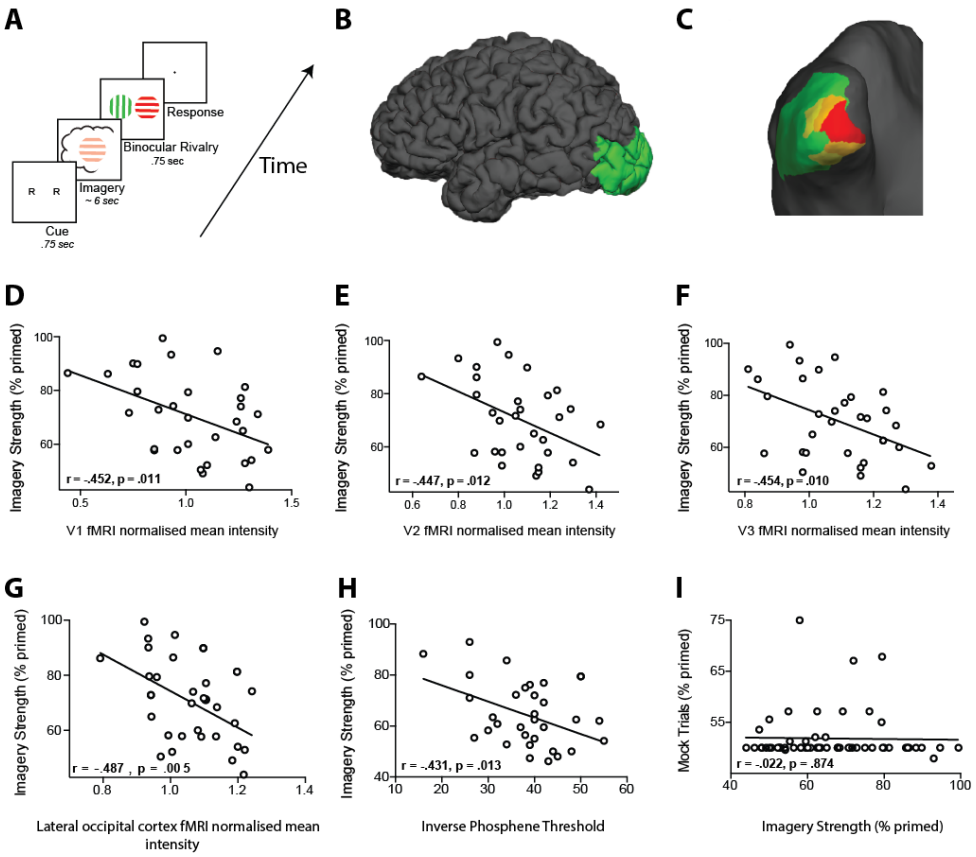

Fig. 1. **A.** Timeline of the basic imagery experiment. Participants were cued to imagine a red-horizontal or a green-vertical Gabor patch for six to seven seconds by the letter R or G (respectively). Following this, they were presented with a brief binocular rivalry display (750ms) and asked to indicate which image was dominant. In the behavioral experiments with the brain-imaging sample and in the final two tDCS experiments, a rating of subjective vividness of the imagery also preceded the binocular rivalry display. **B and C.** Pial (B) and inflated (C) view of the visual areas that showed a significant negative relationship with imagery. Red = V1, Orange = V2, Yellow = V3 and Green = lateral occipital area **D-G.** Correlation between normalized mean fMRI intensity levels in V1, V2, V3 and lateral occipital area and imagery strength. Individuals with lower normalized mean fMRI intensity levels in early visual cortex showed stronger imagery. **H.** Correlation between the inverse phosphene threshold and imagery strength. Individuals with lower cortical excitability in visual cortex tended to have stronger imagery. **I.** Correlation between mock priming scores and real binocular rivalry priming for participants in the fMRI and TMS study. There was no significant association between perceptual priming in real and mock trials. In the scatterplots (D-I), each data point indicates the value of one participant; the bivariate correlation coefficients are included with their respective significance levels.

fMRI activity at rest is influenced by a number of factors other than neural activity, such as non-neuronal physiological fluctuations or scanner noise (Fox and Raichle, 2007). Nonetheless, previous research has shown that the fMRI signal during resting state is strongly reflective of underlying neural activity (Scholvinck et al., 2010, Bianciardi et al., 2009a, Bianciardi et al., 2009b).

Our data are compatible with the hypothesis that the resting levels of early visual cortex activity are negatively related to imagery strength. However, mean fMRI intensity levels are not a commonly used measure, and individual variation in this parameter remains poorly understood. By normalizing the individual fMRI signal levels of our ROIs using the whole brain's signal intensity, we aimed to control for non-neuronal influences that may affect the individual brain in its entirety (e.g. scanner noise, motion etc.). We also excluded the possibility that differences in head size contributed to the relationship between the ROIs' mean fMRI signal levels and individual behavior. Using cortical surface area and volume, respectively, as proxies for head size (Tramo et al., 1998) there was no significant relationships with either the behavioral or fMRI data (all p>.16). Accordingly, partialling these factors out of the correlations did not change the pattern of significant results (all ps<.02).

To further substantiate our observations and rule out other potential confounds that might influence the fMRI data, we next utilized a different methodology that measures induced cortical excitability: transcranial magnetically induced phosphenes. A new sample of 32 participants performed an automated phosphene threshold procedure using transcranial magnetic stimulation (TMS) over early visual cortex (see methods). Visual phosphenes are weak hallucinations caused by TMS applied to visual cortex. The magnetic strength needed to induce a phosphene is a reliable and non-invasive method to measure cortical excitability. In line with the normalized mean fMRI intensity data, we found a significant negative correlation between imagery strength and visual cortex excitability (inverse phosphene threshold: r= -.44, p < .05; Fig.1H). In other words, individuals with lower visual cortex excitability exhibited stronger imagery. Importantly, we also tested the phosphene threshold retest

reliability for our paradigm over two days and found it was a very reliable measure (r = .79, p < .001; see Supplementary Fig.S2B) and the imagery strength re-test was also reliable (r = .62, p < .001; see Supplementary Fig.S2A).

To assess possible effects of a decisional bias, mock rivalry trials were included in all tests of imagery strength (Pearson et al., 2008, Bergmann et al., 2015, Keogh and Pearson, 2011, Keogh and Pearson, 2014)(see Methods). We found no correlation between real binocular rivalry and 'mock priming' (combined fMRI & TMS mock data: r = -.02, p = .87, see Fig.1I). These data, in conjunction with the effects of background luminance, make it unlikely that the relationship between imagery strength and physiology is due to demand characteristics, decisional bias or voluntary rivalry control.

Manipulating visual cortex excitability

The previous data suggest that the excitability of the visual cortex, correlates negatively with imagery strength; that is, participants with lower visual cortex activity tended to have stronger visual imagery. However, these data do not speak to the causal role of early visual cortex in creating strong mental images. If the association between imagery strength and visual cortex activity is causal, manipulating visual cortex excitability should likewise modulate imagery strength.

To assess this hypothesis, we utilized non-invasive transcranial direct current stimulation (tDCS), which can increase or decrease cortical excitability depending on electrode polarity and position (see (Filmer et al., 2014) for review). When the cathode is placed over the cortex, the underlying excitability is decreased, whereas the anode increases excitability. Sixteen new participants underwent both anodal and cathodal stimulation of visual cortex (see Fig.2B for electrode montage) on two separate days (separated by at least twenty-four hours). On each day, participants completed six blocks of the imagery task, two before tDCS, two during tDCS and two post tDCS (see Fig.2A for the experimental timeline). To assess the effect of tDCS on imagery strength, we calculated

difference scores for each participant by subtracting the mean priming rate preceding tDCS from those during and after tDCS (block (n) - (average of two tDCS blocks before stimulation)). Positive values indicate an increase in imagery strength, whereas negative values a decrease. Fig. 2B shows imagery difference scores averaged across all stimulation blocks with 1mA of tDCS stimulation. There was no main effect of tDCS polarity ($F(1,15) = 2.91$, $p = .11$), however, there was a main effect of block, collapsed across tDCS polarity ($F(2.02,30.24) = 7.1$, $p < .001$, Greenhouse-Geisser correction for violation of sphericity, see supplementary figure S6 for graphs separated by block). The interaction between block and polarity was close to significance ($F(3, 45) = 2.46$, $p = .075$) and a post-hoc analysis showed that during the first block of tDCS the cathodal difference score was significantly higher compared to anodal (pairwise comparison $p < .01$, with Bonferroni correction). A Bayesian analysis showed that there were very strong Bayes factors for effects of time (BF = 1360) and an interaction between tDCS polarity and time (BF = 1465.17), suggesting both models are favorable over the null hypothesis.

A

Eye Dominance Test	Pre Test One	Pre Test Two	Test During tDCS one (D1)	Test During tDCS two (D2)	Test Post tDCS one (P1)	Test Post tDCS two (P2)
~ 15 min	~ 7.5 min	~ 7.5 min	~ 7.5 min	~ 7.5 min	~ 7.5 min	~ 7.5 min

B

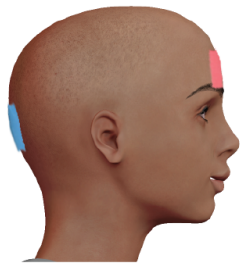

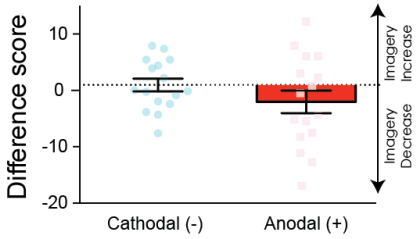

1 mA occipital and supraorbital

C

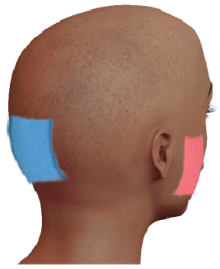

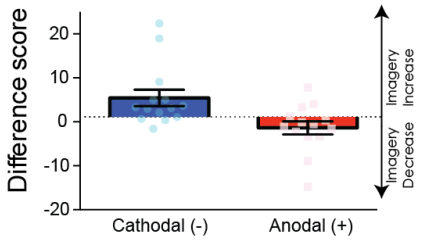

1.5 mA occipital and Cheek

D

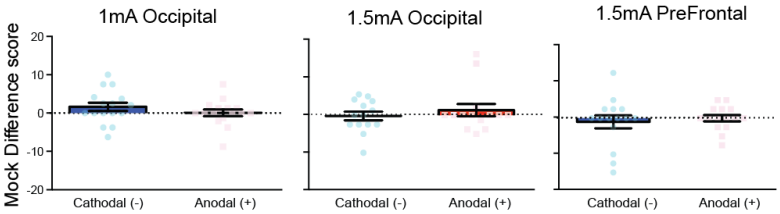

Fig.2. **A.** tDCS experimental timeline**. B.** Effect of visual cortex stimulation on imagery strength at 1mA. The left image shows the tDCS montage, with the active electrode over OZ and the reference electrode on the supraorbital area. The right image shows the effect of cathodal (decreases excitability, blue bars represent mean difference score while blue dots represent each participant's difference score) and anodal (increases excitability, red bars represent mean difference score while red squares represent each individual participant's difference score) stimulation averaged across all tDCS stimulation blocks (D1, D2, P1 and P2). **C.** Effect of visual cortex stimulation on imagery strength at 1.5mA. This experiment was included to control for possible stimulation of the frontal lobes in the first tDCS experiment (**Fig.2B**). To the left: the tDCS montage with the active electrode over OZ and the reference electrode on the right cheek. To the right: the effect of cathodal (blue bars and dots, decrease excitability) and anodal (red bars and squares, increase excitability) stimulation averaged across all blocks during and after tDCS stimulation (D1, D2, P1 and P2).Imagery strength increases in the cathodal stimulation condition, when neural activity is reduced. **D.** Lack of effect on mock priming. We found no change in mock priming scores across the different stimulation blocks in any of the tDCS experiments (left panel = OZ/supraorbital 1mA, middle panel = OZ/cheek 1.5mA, right panel = FzF3/cheek 1.5mA). All error bars show ±SEMs.

We ran a second tDCS study with a higher intensity of 1.5mA, in an attempt to boost the cathodal and anodal effects (see methods). To ensure the findings of the previous tDCS study were not due to the frontal placement of the reference electrode in this study we changed the position of the reference electrode, placing it on the cheek (Fig.2C). Fourteen new participants completed both anodal and cathodal stimulation over two separate days, which resulted in a main effect of tDCS polarity ($F(1,13) = 12.17$, $p < .01$). Imagery strength was significantly higher in the cathodal condition compared to the anodal condition, suggesting that tDCS over visual cortex can increase imagery strength (Fig.2C). There was no main effect of block ($F(3, 39) = .46$, $p = .71$, see supplementary figure S6 for graphs separated by block) or interaction between block and tDCS polarity($F(3, 39) = .16$, $p = .92$). A Bayesian analysis showed strong evidence that the data was driven by the polarity of tDCS (BF = 471.49). Again, the mock data showed no significant difference in 'decisional priming' across the cathodal and anodal conditions, or over experimental blocks for any of the tDCS data (see Fig.2D and supplementary results, all $p > .19$). Taken together, these data provide evidence that tDCS changes visual imagery strength in a polarity-specific way, with probable decreases in visual cortex excitability leading to increased imagery strength.

Although other studies have provided evidence that tDCS does change the excitability of the visual cortex (see (Antal et al., 2003) for example), we wanted to ensure that our specific stimulation paradigm was indeed modulating visual cortex excitability. We ran a separate control study comparing TMS-phosphene thresholds in 16 new subjects before and after the same tDCS paradigm. If our cathodal stimulation is indeed decreasing visual cortex excitability, greater TMS power output would be required to elicit phosphenes post cathodal stimulation, whereas post anodal stimulation we would predict the opposite effect. We found that phosphene thresholds measured immediately after anodal stimulation decreased, whereas after cathodal stimulation phosphene thresholds increased ($t(15) = 2.46$, $p < .05$; see Supplementary Fig. S7). These findings show that our stimulation paradigm changes cortical excitability in the expected direction, i.e.

Cathodal stimulation decreases cortical excitability, whereas anodal stimulation increases activity.

Correlations between frontal cortex excitability and imagery strength

Taken together these data suggest that visual cortex excitability plays a causal role in modulating imagery strength, but how exactly might excitability influence imagery strength? One hypothesis is that hyperexcitability might act as a source of noise in visual cortex that limits the availability or sensitivity of neuronal response to top-down imagery signals, resulting in weaker image-simulations. This hypothesis is supported by behavioral work showing that both imagery and visual working memory can be disrupted by the passive presence of uniform bottom-up afferent visual stimulation (Keogh and Pearson, 2011, Keogh and Pearson, 2014), known to increase neural depolarization in primary visual cortex (Kinoshita and Komatsu, 2001). However, the strength of the top-down imagery-signals arriving at visual cortex should also play a role in governing imagery strength as activity in a brain network including prefrontal areas supports mental image generation (Pearson et al., 2015).

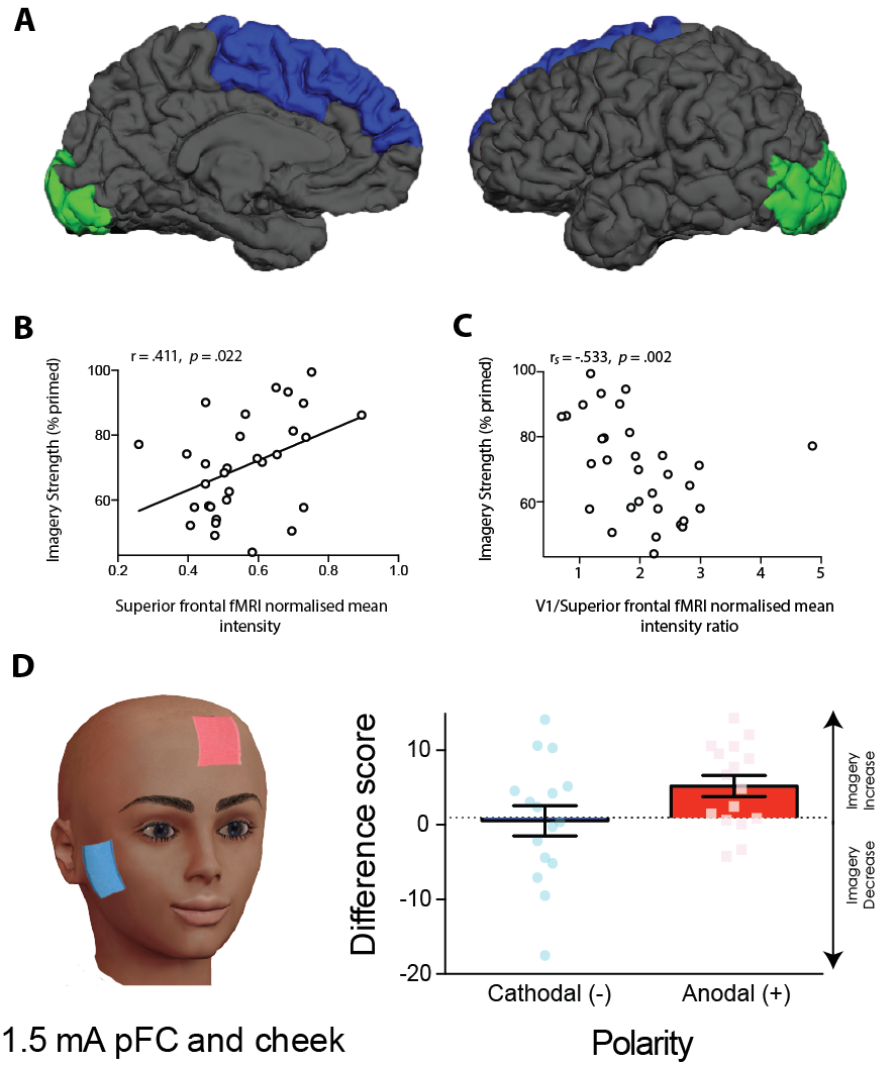

Fig.3*. Correlational and causative data for prefrontal cortex.* **A.** Image shows brain areas correlated with imagery strength (green = early visual areas and lateraloccipital cortex (negative correlation), dark blue = superior frontal areas (positive correlation). **B.** Correlation between superior frontal normalized mean fMRI intensity and imagery strength. **C.** Correlation (Spearman rank) between V1 and superior frontal mean fMRI intensity ratio and imagery strength. **D.** Experimental timeline for tDCS protocol on each day of testing. **E.** Effect of left prefrontal cortex stimulation on imagery strength at 1.5mA. The left image shows the tDCS montage, with the active electrode between Fz and F3 and the reference electrode on the right cheek. The right image shows the effect of cathodal (decrease excitability, blue bars represent mean difference score while blue dots represent each participant's difference score) and anodal (increase excitability, red bars represent mean difference score while red squares represent each individual participant's difference score) stimulation averaged across all blocks during and after tDCS stimulation (D1, D2, P1 and P2). Imagery strength can be seen to increase with anodal stimulation. All error bars show ±SEMs.

As mentioned previously, the whole-brain surface-based analysis of the mean fMRI intensity levels at rest revealed relationships with clusters in both visual cortex and frontal cortex (multiple-comparison corrected; see Supplementary Fig.S4 and Table S2). Additionally, using a ROI-based approach, normalized mean fMRI intensity levels in two frontal areas also showed significant positive relationships with imagery strength: superior frontal cortex (Fig.3A-B dark blue: r = .41, p = .022) and area parsopercularis (r = .38, p = .033; ROIs defined by the Desikan–Killiany atlas), while no other ROI showed a significant positive association.

Manipulating prefrontal cortex excitability

Next we sought to evaluate the effect of modulating neural excitability in prefrontal cortex using tDCS during image generation. The active electrode was placed between F3 and Fz (left frontal cortex), and the reference electrode on the right cheek (Fig.3E for montage). Participants completed both cathodal and anodal conditions (1.5mA) over two separate days (see Fig. 3D for timeline). Interestingly, in contrast to the visual cortex where decreasing excitability led to stronger imagery, we found a trend in the opposite pattern for frontal areas (main effect of tDCS polarity: F(1,15) = 3.81, p = .07,see Fig.3D). There was no main effect of block (F(3,45) = 1.86, p = .15, see Supplementary figure S5 for effects of tDCS separated by block) and no interaction between block and tDCS polarity (F(1.82,27.29) = 1.51, p = .24, Greenhouse-Geisser correction for violation of sphericity; Fig. 3D). However, the Bayesian analysis of the frontal data showed a substantial Bayes factor for polarity of tDCS (BF = 7.45), suggesting that the observed data were more likely due to the polarity of the tDCS than chance.

The joint role of visual and frontal cortex activity in visual imagery strength

Beyond the individual roles of prefrontal and visual cortex in forming mental images, evidence suggests that both areas can act together as part of an imagery network (Ostby et al., 2012, Schlegel et al., 2013). Hence, we combined

the whole-brain normalized mean fMRI intensity scores from the two areas (frontal and visual) and related their ratio to imagery strength. We found that the ratio of V1 to superior frontal predicted the strength of visual imagery (Spearman rank: r_s = -.53, p = .002, see Fig.3C). This effect also held when controlling for the Euklidean distance between the two areas (partial Spearman rank: r_s = -.54, p = .002). Hence, participants with both comparatively lower levels of visual cortex normalized mean intensity and higher frontal levels had stronger imagery.

To further rule out the possibility that cortical connectivity might be driving this fronto-occipital excitability relationship, we analyzed the individual functional connectivity of the same two areas for each participant, that is, the degree to which the BOLD signals in each area correlate over time. The functional connectivity did not significantly predict imagery strength (r = -.24, p = .19). This suggests that the combination of highly active frontal areas and low visual cortex excitability might present an optimal precondition for strong imagery creation, irrespective of the temporal coupling of their activity.

Discussion

Perhaps as far back as Plato, but overtly since the 1880s philosophers, scientists and the general populace have wondered why the human imagination differs so profoundly from one individual to the next. Indeed, this question has recently gained fresh notability and attention with the introduction and classification of the term aphantasia to describe individuals who self-report no imagery at all (Zeman et al., 2015). Here we show the first evidence that pre-existing levels of neural excitability and spontaneous resting activity in visual cortex and frontal areas can influence the strength of mental representations. Our data indicate that participants with lower excitability in visual cortex have stronger imagery. Furthermore, we provide causative evidence, using tDCS over both visual and frontal cortex, that imagery strength is contingent on the neural excitability of these areas.

A plethora of imagery research has demonstrated evoked and content specific BOLD responses in early and later visual cortex when individuals form a mental image (Naselaris et al., 2015, Cui et al., 2007, Pearson et al., 2015). Here however, we took a different approached by examining the individual variation in brain physiology that might form the preconditions for strong or weak imagery. This endeavor, by definition required a non-event related design. Interestingly, such non-event related designs utilizing inter-individual differences are now commonly used to mechanistically link human cognition and brain function or anatomy (Kanai and Rees, 2011). Our results add to this growing body of research, which demonstrates that pre-existing brain activity parameters can fundamentally influence mental performance.

Specifically, these findings could be explained by hyperexcitability acting as a source of noise in visual cortex, which, when reduced, allows a higher signal-to-noise ratio in visual cortex and thus stronger imagery. This hypothesis is in line with findings from related research. Grapheme-color synesthesia can also be enhanced by reducing visual excitability via tDCS (Terhune et al., 2015). It has been proposed that this effect is likewise due to increased signal-to-noise (Terhune et al., 2015). In addition, the expectation of a visual stimulus leads to an imagery-like stimulus template, reduced activity in V1 and improved stimulus decoding by pattern classifiers (Kok et al., 2013). Similarly, reduced early visual cortex activity increases the likelihood of visual hallucinations in a subsequent detection task (Pajani et al., 2015). Further, behavioral data suggests that the presence of uniform afferent visual stimulation during mental image generation and visual working memory storage (Keogh and Pearson, 2011, Keogh and Pearson, 2014) attenuates sensory strength and retention (Keogh and Pearson, 2011, Keogh and Pearson, 2014, Pearson et al., 2008). The convergence of these data appear to indicate that 'background' neural noise in sensory cortices may play an important role in modulating the strength of mental representations.

A recent study (Bergmann et al., 2015) found that individuals with a smaller V1 could form stronger mental images, which might be caused by the effective increase in control of top-down signals enabled by a smaller primary

visual cortex. Interestingly, recent data suggests there may also be anatomical reciprocity between V1 and prefrontal cortex in humans (Song et al., 2011). Our present results suggest there may also be functional reciprocity in terms of neural excitability between the two regions.

Over the last 30 years empirical work has demonstrated many commonalities between imagery and visual perception (see (Pearson et al., 2015) for a review). However, the two experiences have clear phenomenological differences between them. Our findings suggest a possible novel dissociation between mental imagery and visual perception, as perceptual sensitivity is associated with higher levels of visual cortex excitability, whereas our results suggest the opposite for mental imagery; stronger imagery is associated with lower visual excitability.

Our data suggest that neural excitation in visual and pre-frontal cortices, and the interplay between the two, play a key role in governing the strength of mental imagery. Our observations may also have strong clinical applications: In many mental disorders imagery can become uncontrollable and traumatic, however new research shows that mental imagery can also be harnessed specifically to treat these disorders (Pearson et al., 2015). Likewise, disorders that involve visual hallucinations such as schizophrenia and Parkinson's disease are both associated with stronger or more vivid mental imagery (Shine et al., 2015, Sack et al., 2005, Matthews et al., 2014). Additionally, it has recently been suggested that the balance between top-down and bottom-up information processing may be a crucial factor in the development of psychosis, with early and psychosis prone individuals displaying a shift in information processing towards top-down influences over bottom-up sensory input (Teufel et al., 2015). Our data indicate it may be possible to treat symptomatic visual mental content by reducing its strength via non-intrusively manipulating cortical excitability. Alternatively, we may be able to 'surgically' boost mental image simulations specifically during imagery-based treatments, resulting in better treatment outcomes. Further research on longer lasting stimulation protocols is needed to assess its therapeutic potential.

Experimental Procedures

Participants

All participants were right-handed and had normal or corrected-to-normal vision. None of them had a history of psychiatric or neurological disorders.

Brain imaging sample: 32 individuals (age range: 18 - 36 years, median: 25.5; 13 males) participated in the fMRI resting-state and retinotopic mapping measurements and in the behavioral experiment. One participant was excluded from data analysis because of misunderstanding the task instructions in the behavioral imagery task. Of the remaining 31 individuals, a subsample of 24 also participated in the luminance condition of the behavioral experiment, which was conducted in a separate session. Participants were reimbursed for their time at a rate of 15€ per hour. Written informed consent was obtained from all participants and the ethics committee of the Max Planck Society approved the study.

TMS samples: All participants in both the TMS and tDCS studies had normal or corrected to normal vision, no history of any neurological or mental health issues or disorders, no history of epilepsy or seizures themselves or their immediate family, no history of migraines and no metal implants in the head or neck region. We aimed to collect phosphene thresholds from 30-35 participants, which would give us power of around 80-85% for a moderate correlation. A total of thirty-seven participants participated in this study for money ($30 per hour) or course credit, five participants were excluded due to an inability to produce reliable phosphenes. Of the remaining thirty-two participants 15 were female, age range: 18-30). Written informed consent was obtained from all participants and the ethics committee of the University of New South Wales approved the study.

TDCS samples: For all tDCS experiments we aimed to collect data from 15-20 participants, as most tDCS studies examining effects on cognition have found significant effects with this range of participants (See for examples: (Javadi and

Cheng, 2013, Strobach et al., 2015, Manuel et al., 2014, Javadi et al., 2012)). A priori we chose a cut-off of 33% of trials being mixed as an exclusion criteria. Participants with imagery scores below 45% were removed as their priming scores approached a floor, e.g. their imagery could not get any lower and as such we would not be able to observe decreases in imagery even if they occurred (two participants were excluded). For the first tDCS experiment (1mA, Occipital and Supraorbital) a total of twenty-one subjects participated for money or course credit. Five participants were excluded from our analysis as the number of usable trials was small due to too many reported mixed rivalry percepts (more than a third of trials, three participants). Of the remaining sixteen participants 7 were female, and the age range was 18-32.

For the second tDCS experiment (1.5mA, Occipital and Cheek) a total of fifteen subjects participated for course credit. One participant was excluded as they did not complete both sessions of the experiment. Of the remaining fourteen participants 6 were female, age range 18-26.

For the final tDCS experiment (1.5mA, left prefrontal and cheek) twenty-three participants participated in the study for course credit. Five participants were excluded from the analysis for reporting too many mixed percepts, using the above-mentioned criteria. Two further participants were excluded for not completing both sessions of the study (attrition). One participant was removed for priming lower than 45%. Of the remaining sixteen participants 8 were female, and the age range was 18-25 years.

All subjects participated in this study for course credit or money *$30 AUD per hour). Written informed consent was obtained from all participants and the ethics committee of the University of New South Wales approved the studies.

tDCS modulation of phosphene thresholds control study: A total of twenty-nine subjects participated in this study for money ($30 AUD per hour) or course credit. Of these 29 participants thirteen were excluded due to a number of strict exclusion criteria in regards to reliability of phosphene thresholds. If

participants reported phosphenes in the wrong visual hemi-field (e.g. left visual hemisphere was stimulated and participants reported phosphenes in the left visual hemi-field) their data was excluded (N = 2). If participants blinked during the rapid estimation of phosphene thresholds (REPT) procedure their data was also removed from analysis (N = 3). Additionally, if a participant's phosphene thresholds were greater than 10% different from day one to day two their data was removed from the analysis (N = 3). A participant's data was also removed if the REPT procedure took longer than five minutes to set up after tDCS stimulation (N = 1). 3 participants were also removed due to technical issues with the tDCS machine exceeding voltages on one of the days (N = 2) or the REPT Matlab procedure experiencing errors (N = 1). One participant was removed due to attrition (N = 1). This resulted in 16 participants' data being analysed (8 female, age range 18-25). Written informed consent was obtained from all participants and the ethics committee of the University of New South Wales approved the study.

TMS Phosphene threshold reliability study: This sample consisted of the same twenty-nine subjects that participated in the control study to test tDCS modulation of phosphene thresholds. Exclusion criteria were the same as stated above, with the exception that those participants whose phosphene thresholds were greater than 10% different from day one to day two their data were *not* removed from the analysis (N=3); the study also included those 2 participants where technical issues with the tDCS machine had prevented their inclusion in the tDCS modulation study. This resulted in 21 participants data being analysed (11 female, age range 18-25).

Written and informed consent was obtained for all participants and the ethics committee of the University of New South Wales approved all the TMS and tDCS studies.

Behavioral measurements

Apparatus

Brain imaging sample: Participants sat in a darkened room with dark walls, wearing red-green anaglyph glasses for the binocular rivalry imagery paradigm. Their head position was stabilized with a chin rest and the distance to the screen was 75 cm. The stimuli were presented on a CRT monitor (HP p1230; resolution, 1024 x 768 pixels, refresh rate: 150 Hz; visible screen size: 30° x 22.9°) and controlled by MATLAB R2010a (The MathWorks, Natick, MA) using the Psychophysics Toolbox extension (Brainard, 1997, Pelli, 1997, Kleiner et al., 2007), running on Mac OSX, version 10.7.4.

TMS/tDCS sample: All experiments were performed in a blackened room on a 27 inch iMac with a resolution of 2560x1440 pixels, with a frame rate of 60Hz. A chin rest was used to maintain a fixed viewing distance of 57cm. Participants wore red-green anaglyph glasses throughout all experiments.

Stimuli

Brain imaging sample: The circular Gaussian-windowed Gabor stimuli were presented centrally, spanning a radius of 4.6° around the fixation point in visual angle (thereby covering a diameter of 9.2°), one period subtending a length of 1.2°. The peak luminance starting value was ~0.71 cd/m^2 for the red horizontal grating, and ~0.73 cd/m^2 for the green vertical grating, which was then individually adjusted for each participant to compensate for eye dominance (see further below).

TMS/tDCS sample: The binocular rivalry stimuli were presented in a Gaussian-windowed annulus around the bull's eye and consisted of a red-horizontal (CIE X = .579 Y = .369 and green-vertical (CIE X = .269 Y = .640), Gabor patch, 1 cycle/°,

with a diameter of 6° and a mean luminance of 6.06cd/m$^{2.}$ The background was black throughout the entire experiment.

Mock trials: Mock rivalry displays were presented on 10% of trials in the behavioral measurements with the brain imaging sample, 25% of trials in the first two tDCS experiments as well as the TMS experiment, and in 12.5% of the third tDCS experiment to assess demand characteristics. The mock displays consisted of a spatial mix of a red-horizontal and green-vertical Gabor patch (50/50% or 25/75%). The mock display was spatially split with a blurred edge and the exact path of the spatial border changed on each trial based on a random function. Otherwise the mock rivalry displays had the same parameters as the Gabor patches described in the previous paragraph.

Procedure

Participants first underwent a previously documented eye dominance task, which has been shown to reliably measure the sensory strength of mental imagery through its impact on subsequent binocular rivalry perception (Keogh and Pearson, 2011, Keogh and Pearson, 2014, Pearson, 2014, Pearson and Brascamp, 2008, Sherwood and Pearson, 2010, Pearson et al., 2008, Rademaker and Pearson, 2012), thus avoiding any reliance on self-report questionnaires or compound multi-feature tasks. Previous work has demonstrated that when individuals imagine a pattern or are shown a weak perceptual version of a pattern, they are more likely to see that pattern in a subsequent brief binocular rivalry display (see (Pearson, 2014) for a review). Longer periods of imagery generation or weak perceptual presentation increase the probability of perceptual priming of subsequent rivalry (Brascamp et al., 2007, Pearson et al., 2008). For this reason, the degree of imagery priming has been taken as a measure of the sensory strength of mental imagery(Keogh and Pearson, 2011, Keogh and Pearson, 2014, Pearson, 2014, Pearson et al., 2008, Sherwood and Pearson, 2010, Pearson and Brascamp, 2008, Rademaker and Pearson, 2012). This measure of imagery strength has been shown to be both retinotopic location- and spatial orientation-specific (Pearson and Brascamp, 2008,

Bergmann et al., 2015), is closely related to phenomenal vividness (Rademaker and Pearson, 2012, Chang et al., 2013), is reliable when assessed over days (Rademaker and Pearson, 2012) or weeks (Bergmann et al., 2015), is contingent on the imagery generation period (therefore not due to any rivalry control (Sherwood and Pearson, 2010)) and can be dissociated from visual attention (Pearson et al., 2008).

At the beginning of each trial of the imagery experiment, participants were presented with a letter 'R' or 'G' which indicated which image they were to imagine (R = red-horizontal Gabor patch, G = green-vertical Gabor patch). Participants then imagined the red or green pattern for either six (tDCS and TMS experiments) or seven seconds (behavioral measurements of the brain imaging sample). Following this imagery period, the binocular rivalry display appeared for 750ms and participants indicated which image was dominant by pressing '1' for mostly green, '2' for a mix and '3' for mostly red. During the behavioral measurements of the brain imaging sample and in the final two tDCS experiments, on-line ratings of imagery vividness were collected by having participants rate the vividness of the image they had created (on a scale of '1' = least vivid to '4' = most vivid) on each trial after the imagery period and before the binocular rivalry display. For the tDCS experiments there were no effects for mean subjective ratings of imagery vividness (see Supplementary Fig. S7 and S8). For the subjective vividness ratings acquired in the brain imaging sample, we conducted a whole-brain surface-based analysis of the fMRI resting-state data (see Methods and Supplementary Fig.S6 and Table S3). During the imagery experiment where background luminance was included, the procedure was the same as the basic imagery experiment, except that during the imagery period, the background ramped up and down (1s up, 1s down, to avoid visual transients) to a yellow color (the mean of the two binocular rivalry colors). Throughout all imagery experiments, participants were asked to maintain fixation on a bulls-eye fixation point in the center of the screen.

Brain imaging sample. Participants completed 100 trials of the standard imagery paradigm per session (outside the scanner). The behavioral test session was

repeated after an average of ~2 weeks with each participant. All of the runs were divided into blocks of 33 trials, and participants were asked to take a rest in between. In one participant, there was a strong perceptual bias for 1 of the 2 rivalry patterns in the first session due to incorrectly conducted eye dominance adjustments. Therefore, only the data set from the second session of this participant was used for later analysis. The retests demonstrated a very high retest reliability of the imagery strength measure (r = .877, p < .001). In the luminance condition, which was tested on a subsample of the original sample in another session, the participants completed 50 trials. The data from both conditions were checked for normal distribution using Shapiro-Wilk normality test. No violation of the normality assumption was detected (both p > .52).

TMS/tDCS samples. For the TMS study, participants completed one block of 40 imagery trials. In all tDCS experiments, participants completed a total of 40 trials for each block resulting in a total of 480 trials across the two days of testing.

Control tDCS modulation of phosphene thresholds experiment. Participants completed both the anodal and cathodal stimulation across two days separated by at least 24 hours, the order of which was randomized and counterbalanced across participants. Participants completed a memory or psychophysical task (both of which are not relevant to the current study) followed by the automated REPT phosphene threshold procedure prior to tDCS stimulation. Following this, participants completed two blocks of the imagery task (see main texts methods for full description of procedure and stimuli) with fifteen minutes of cathodal or anodal stimulation. Immediately after the tDCS stimulation participants completed the automated REPT procedure again.

Neuroimaging experiments

All neuroimaging data were acquired at the Brain Imaging Center Frankfurt am Main, Germany. The scanner used was a Siemens 3-Tesla Trio (Siemens, Erlangen, Germany) with an 8-channel head coil and a maximum gradient strength of 40 mT/m. Imaging data were acquired in one or two scan sessions per participant, which were conducted on the same day.

Anatomical imaging: For anatomical localization and coregistration of the functional data, T1-weighted anatomical images were acquired first using an MP-RAGE sequence with the following parameters: TR = 2250 ms, TE = 2.6 ms, flip angle: 9°, FoV: 256 mm, resolution = 1 x 1 x 1 mm^3.

fMRI Retinotopic mapping measurement and analysis

This procedure has already been described in previous studies (Bergmann et al., 2015, Bergmann et al., 2014, Genç et al., 2015). A gradient-recalled echo-planar (EPI) sequence with the following parameter settings was applied: 33 slices, TR = 2000 ms, TE = 30 ms, flip angle = 90°, FoV = 192 mm, slice thickness = 3 mm, gap thickness = 0.3 mm, resolution = 3 x 3 x 3 mm^3. A MR-compatible goggle system with two organic light-emitting-diode displays was used for presentation of the stimuli (MR Vision 2000; Resonance Technology Northridge, CA), which were generated with a custom-made program based on the Microsoft DirectX library (Muckli et al., 2005). The maximal visual field subtended 24° vertically and 30° horizontally.

Retinotopic mapping procedure. To map early visual cortices V1, V2 and V3, our participants completed two runs, a polar angle mapping and an eccentricity mapping run. The rationale of this approach has already been described elsewhere (Sereno et al., 1995, Wandell et al., 2007). Polar angle mapping: For the mapping of boundaries between areas, participants were presented with a black and white checkerboard wedge (22.5° wide, extending 15° in the periphery) that slowly rotated clockwise around the fixation point in front of a grey background. In cycles of 64 s, it circled around the fixation point 12 times at a speed of 11.25 in polar angle/volume (2 s). Eccentricity mapping: To map bands of eccentricity on the cortical surface to the corresponding visual angles from the center of gaze, our participants were presented with a slowly expanding flickering black and white checkerboard ring in front of a grey background (flicker rate: 4 Hz). The ring started with a radius of 1° and increased linearly up to a radius of 15°. The expansion cycle was repeated 7

times, each cycle lasting 64 s. The participants' task in both mapping experiments was to maintain central fixation.

Retinotopic mapping data analysis. We used FreeSurfer's surface-based methods for cortical surface reconstruction from the T1-weighted image of each participant (Dale et al., 1999, Fischl et al., 1999) (http://surfer.nmr.mgh.harvard.edu/fswiki/RecommendedReconstruction). FSFAST was applied for slice time correction, motion correction and co-registration of the functional data to the T1-weighted anatomical image. Data from the polar angle and eccentricity mapping experiment were analysed by applying a Fourier transform to each voxel's fMRI time series to extract amplitude and phase at stimulation frequency. Color-encoded F-statistic maps were then computed, each color representing a response phase whose intensity is an F-ratio of the squared amplitude of the response at stimulus frequency divided by the averaged squared amplitudes at all other frequencies (with the exception of higher harmonics of the stimulus frequency and low frequency signals). The maps were then displayed on the cortical surface of the T1-weighted image. Boundaries of areas V1, V2 and V3 were then estimated manually for each participant on the phase-encoded retinotopic maps up to an eccentricity of 7.2°.

fMRI Resting-state data acquisition and analysis

fMRI resting-state data acquisition. The data were collected using a gradient-re-called echo-planar imaging (EPI) sequence with the following parameters: TR = 2000 ms, TE = 30 ms, flip angle = 90°, FoV = 192 mm, slice thickness = 3 mm, number of slices = 33, gap thickness = 0.3 mm, voxel size = 3 x 3 x 3 mm^3. During the scans, the screen remained grey and participants had no further instruction but to keep their eyes open and fixate a cross in the center of the grey screen.

fMRI resting-state data analysis: whole-brain surface-based group analysis. For a first assessment of the relationship between behavior and the fMRI data, we ran whole-brain analyses with the mean fMRI intensity data using a surface-based

group analysis in FreeSurfer. Preprocessing of the functional data was done using FSFAST, which included slice time correction, motion correction and co-registration to the T1-weighted anatomical image. No smoothing was applied, and the first 2 volumes of the fMRI measurement were discarded. As a next step, each individual's mean fMRI intensity data were nonlinearly resampled to a common group surface space (fsaverage), which allows for comparisons at homologous points within the brain. Following this, a general linear model fit to explain the individual behavioral data by the individual mean fMRI intensity levels was computed vertex-wise using an uncorrected threshold of $P < 0.05$. Correction for multiple comparisons was done using a pre-cached Monte Carlo Null-Z simulation with 10 000 iterations and a cluster-wise probability threshold of $P < 0.05$. In addition, as we had also collected subjective vividness ratings in the brain imaging sample (see Procedure), we also ran the equivalent whole brain analysis for the vividness ratings, using each individual's mean vividness (see Supplementary Fig .S6 and Supplementary Table S3). As already described in our previous study (Bergmann et al., 2015), the subjective vividness values of two individuals were extreme, leading to a violation of the normal distribution assumption. As normality is necessary for the general linear model fit (Shapiro-Wilk normality test: $W(31) = .885$, $p = .003$), the vividness ratings of these two individuals were excluded in the whole brain analysis.

fMRI resting-state data analysis: ROI-based approach. The fMRI resting-state data were first preprocessed individually for each participant using the preprocessing steps implemented in FSL's MELODIC Version 3.10 (http://fsl.fmrib.ox.ac.uk/fsl/fslwiki/MELODIC), which included motion and slice time correction, high-pass temporal filtering with a cut-off point at 200 seconds and linear registration to the individual's T1 anatomical image and to MNI 152 standard space. No spatial smoothing was applied. The first two of the 280 volumes of the measurement were discarded. To compute fMRI mean intensity of the early visual cortex in each individual's subject space, delineations of the areas were first converted from anatomical to functional space in each individual. To ensure that the conversion had not produced overlaps between areas V1-V3, the volumes were subsequently subtracted from each other. Time

courses of V1-V3 were then determined to compute their mean intensity across time. To determine mean intensity for other brain areas, we relied on the gyral-based Desikan–Killiany Atlas (Desikan et al., 2006). To ensure that there was no overlap between posterior atlas-defined areas and the retinotopically mapped early visual cortex, which would result in the mean intensity of these areas being partly computed from the same voxels, the volumes of the retinotopically mapped areas were also subtracted from the adjacent atlas-defined areas; the fMRI mean intensity of the atlas-defined areas was then determined from the remainder of these. The estimates of fMRI mean intensity of the atlas- and retinotopically mapped areas (Fox and Raichle, 2007) were normalized by subtracting the whole brain's mean intensity from the area's mean intensity, divided by the standard deviation of the whole brain's mean intensity.

Like the behavioral data, the normalized mean intensity values were checked for normal distribution using Shapiro-Wilk normality test. None of the retinotopically mapped early visual cortices showed a violation of the normal distribution (all $p > .20$). Of the 34 atlas-defined areas, the normalized mean fMRI intensities of 4 areas showed a violation of the normal distribution assumption ($p < .05$; fusiform, inferiortemporal, parstriangularis and postcentral area). For this reason, the relationships with behavior were also computed using Spearman rank correlations. Like with Pearson product moment correlations, none of the intensities of these areas had a significant relationship with behaviour (all $p > .20$). The ratio of V1 and superiorfrontal mean intensities showed a violation of the normal distribution assumption ($W(31) = .919$, $p = .022$) due to one extreme value (subject S8). Therefore, Spearman rank correlation (r_s) was used to compute the relationship with behavior. To further examine the possibility that temporal coupling between V1 and superiorfrontal cortex might account for their inverse relationship with behavior, we also computed each individual's functional connectivity of these two regions by calculating the time-wise correlation of their resting-state signals in each individual. As the functional connectivity data did not violate the normal distribution assumption (Shapiro-Wilk normality test , $p = .497$), Pearson product moment correlation was used to examine the relationship with behavior.

Phosphene Threshold Determination

Phosphene thresholds were obtained using single pulse TMS with a butterfly shaped coil (Magstim Rapid^2, Carmarthenshire, UK). The coil was placed centrally and approximately 2 cm above the inion. To obtain each participant's phosphene threshold, we used the previously documented automated rapid estimation of phosphene thresholds (REPT) (Abrahamyan et al., 2011). This REPT procedure uses a Bayesian adaptive staircase approach to find the 60% phosphene threshold of each participant.

During the REPT procedure participants were seated in front of a computer screen with a piece of black cardboard with white numbered quadrants covering the monitor. Participants received 30 pulses, of varying intensities, which were delivered automatically by the machine when the participant pressed the space key (self paced). After each pulse participants were instructed to indicate if they had seen a phosphene by pressing the left ('no I did not see a phosphene') or right ('yes I did see a phosphene') shift keys.

Transcranial direct current stimulation

tDCS was delivered by a battery driven portable stimulator (Neuroconn, Ilmenau, Germany) using a pair of 6 x 3.5 cm rubber electrodes in two saline soaked sponges.

Three different montages were used across the different experiments. In experiment 1 the active electrode was placed over Oz while the reference electrode was placed over the midline supraorbital area (see Fig.2B). In experiment 2 the active electrode was placed over Oz and the reference electrode was placed on the right cheek (see Fig.2C). In experiment 3 the active electrode was placed between F3 and Fz while the reference electrode was placed over the right cheek (see Fig.3E).

Each participant received both anodal and cathodal stimulations for a total of thirty minutes (fifteen minutes anodal, fifteen minutes cathodal) in two separate experimental sessions separated by a washout period of at least 24 hours, the order of which was randomized and counterbalanced across participants. The experimenter was not blind to which polarity condition the participant was in from day to day.

In experiment 1 the intensity used for stimulation was 1 mA. Here, a cathodal effect was observed however no anodal effect was seen. To ensure that our lack of an effect with the anodal stimulation was not due to the intensity of the tDCS stimulation being too low (previous studies have demonstrated that the anodal effect may need higher intensities to elicit a result than the cathodal effect (Antal et al., 2006)) we increased the tDCS intensity to 1.5 mA in both experiment 2 and 3.

In the control tDCS modulation of phosphene thresholds experiment, the tDCS parameters were the same as in experiment 2. The intensity of the stimulation was set to 1.5mA and the active electrode placed over Oz and the reference electrode on the right cheek (see main text methods section and Fig. 2.C.)

Statistical analysis of tDCS and TMS data

All ANOVA's and t-tests were run in the SPSS (IBM, Armonk), and the Bayesian analysis was computed using JASP (JASP Team (2016). JASP (Version 0.8.0.0)[Computer software]).

Author Contributions: JB collected and analyzed all of the MRI data. RK collected and analyzed all of the tDCS and TMS data. JB, JP and RK wrote the manuscript.

Acknowledgements: We thank Wolf Singer for his support in the project and for his helpful comments on the manuscript. We would also like to thank Roger Koenig for helpful comments. JP is supported by Australian NHMRC grants APP1024800, APP1046198 and APP1085404 and a Career Development Fellowship APP1049596 and ARC discovery projects DP140101560 and DP160103299. An International Postgraduate Research Scholarship and a Brain Sciences UNSW PhD Top Up Scholarship supported JB. RK was supported by an Australian Postgraduate Award.

References

ABRAHAMYAN, A., CLIFFORD, C. W., RUZZOLI, M., PHILLIPS, D., ARABZADEH, E. & HARRIS, J. A. 2011. Accurate and rapid estimation of phosphene thresholds (REPT). *PLoS One,* 6**,** e22342.

ANTAL, A., KINCSES, T. Z., NITSCHE, M. A. & PAULUS, W. 2003. Manipulation of phosphene thresholds by transcranial direct current stimulation in man. *Exp Brain Res,* 150**,** 375-8.

ANTAL, A., NITSCHE, M. A. & PAULUS, W. 2006. Transcranial direct current stimulation and the visual cortex. *Brain Res Bull,* 68**,** 459-63.

BERGMANN, J., GENC, E., KOHLER, A., SINGER, W. & PEARSON, J. 2014. Neural Anatomy of Primary Visual Cortex Limits Visual Working Memory. *Cereb Cortex*.

BERGMANN, J., GENC, E., KOHLER, A., SINGER, W. & PEARSON, J. 2015. Smaller Primary Visual Cortex Is Associated with Stronger, but Less Precise Mental Imagery. *Cereb Cortex*.

BIANCIARDI, M., FUKUNAGA, M., VAN GELDEREN, P., HOROVITZ, S. G., DE ZWART, J. A. & DUYN, J. H. 2009a. Modulation of spontaneous fMRI activity in human visual cortex by behavioral state. *Neuroimage,* 45**,** 160-8.

BIANCIARDI, M., FUKUNAGA, M., VAN GELDEREN, P., HOROVITZ, S. G., DE ZWART, J. A., SHMUELI, K. & DUYN, J. H. 2009b. Sources of functional magnetic resonance imaging signal fluctuations in the human brain at rest: a 7 T study. *Magn Reson Imaging,* 27**,** 1019-29.

BRAINARD, D. H. 1997. The psychophysics toolbox. *Spatial Vision,* 10**,** 433-436.

BRASCAMP, J. W., KNAPEN, T. H., KANAI, R., VAN EE, R. & VAN DEN BERG, A. V. 2007. Flash suppression and flash facilitation in binocular rivalry. *J Vis,* 7**,** 12 1-12.

CHANG, S., LEWIS, D. E. & PEARSON, J. 2013. The functional effects of color perception and color imagery. *J Vis,* 13.

CUI, X., JETER, C. B., YANG, D., MONTAGUE, P. R. & EAGLEMAN, D. M. 2007. Vividness of mental imagery: individual variability can be measured objectively. *Vision Res,* 47**,** 474-8.

DALE, A. M., FISCHL, B. & SERENO, M. I. 1999. Cortical surface-based analysis. I. Segmentation and surface reconstruction. *Neuroimage,* 9**,** 179-94.

DESIKAN, R. S., SEGONNE, F., FISCHL, B., QUINN, B. T., DICKERSON, B. C., BLACKER, D., BUCKNER, R. L., DALE, A. M., MAGUIRE, R. P., HYMAN, B. T., ALBERT, M. S. & KILLIANY, R. J. 2006. An automated labeling system for

subdividing the human cerebral cortex on MRI scans into gyral based regions of interest. *Neuroimage,* 31**,** 968-80.

FILMER, H. L., DUX, P. E. & MATTINGLEY, J. B. 2014. Applications of transcranial direct current stimulation for understanding brain function. *Trends Neurosci,* 37**,** 742-53.

FISCHL, B., SERENO, M. I. & DALE, A. M. 1999. Cortical surface-based analysis. II: Inflation, flattening, and a surface-based coordinate system. *Neuroimage,* 9**,** 195-207.

FOX, M. D. & RAICHLE, M. E. 2007. Spontaneous fluctuations in brain activity observed with functional magnetic resonance imaging. *Nat Rev Neurosci,* 8**,** 700-11.

GENÇ, E., BERGMANN, J., SINGER, W. & KOHLER, A. 2015. Surface area of early visual cortex predicts individual speed of traveling waves during binocular rivalry. *Cereb Cortex,* 25**,** 1499-508.

ISHAI, A. & SAGI, D. 1995. Common mechanisms of visual imagery and perception. *Science,* 268**,** 1772-4.

JAVADI, A. H. & CHENG, P. 2013. Transcranial direct current stimulation (tDCS) enhances reconsolidation of long-term memory. *Brain Stimul,* 6**,** 668-74.

JAVADI, A. H., CHENG, P. & WALSH, V. 2012. Short duration transcranial direct current stimulation (tDCS) modulates verbal memory. *Brain Stimul,* 5**,** 468-74.

KANAI, R. & REES, G. 2011. The structural basis of inter-individual differences in human behaviour and cognition. *Nat Rev Neurosci,* 12**,** 231-42.

KEOGH, R. & PEARSON, J. 2011. Mental imagery and visual working memory. *PLoS One,* 6**,** e29221.

KEOGH, R. & PEARSON, J. 2014. The sensory strength of voluntary visual imagery predicts visual working memory capacity. *J Vis,* 14.

KINOSHITA, M. & KOMATSU, H. 2001. Neural representation of the luminance and brightness of a uniform surface in the macaque primary visual cortex. *J Neurophysiol,* 86**,** 2559-70.

KLEINER, M., BRAINARD, D. H. & PELLI, D. G. 2007. What's new in Psychtoolbox-3? *Perception,* 36 ECVP Abstract Supplement 14.

KOK, P., BROUWER, G. J., VAN GERVEN, M. A. & DE LANGE, F. P. 2013. Prior expectations bias sensory representations in visual cortex. *J Neurosci,* 33**,** 16275-84.

KOSSLYN, S. M., THOMPSON, W. L. & ALPERT, N. M. 1997. Neural systems shared by visual imagery and visual perception: a positron emission tomography study. *Neuroimage,* 6**,** 320-34.

MANUEL, A. L., DAVID, A. W., BIKSON, M. & SCHNIDER, A. 2014. Frontal tDCS modulates orbitofrontal reality filtering. *Neuroscience,* 265**,** 21-7.

MATTHEWS, N. L., COLLINS, K. P., THAKKAR, K. N. & PARK, S. 2014. Visuospatial imagery and working memory in schizophrenia. *Cogn Neuropsychiatry,* 19**,** 17-35.

MUCKLI, L., KOHLER, A., KRIEGESKORTE, N. & SINGER, W. 2005. Primary visual cortex activity along the apparent-motion trace reflects illusory perception. *PLoS Biol,* 3**,** e265.

NASELARIS, T., OLMAN, C. A., STANSBURY, D. E., UGURBIL, K. & GALLANT, J. L. 2015. A voxel-wise encoding model for early visual areas decodes mental images of remembered scenes. *Neuroimage,* 105**,** 215-28.

OSTBY, Y., WALHOVD, K. B., TAMNES, C. K., GRYDELAND, H., WESTLYE, L. T. & FJELL, A. M. 2012. Mental time travel and default-mode network functional connectivity in the developing brain. *Proc Natl Acad Sci U S A,* 109**,** 16800-4.

PAJANI, A., KOK, P., KOUIDER, S. & DE LANGE, F. P. 2015. Spontaneous Activity Patterns in Primary Visual Cortex Predispose to Visual Hallucinations. *J Neurosci,* 35**,** 12947-53.

PEARSON, J. 2014. New Directions in Mental-Imagery Research: The Binocular-Rivalry Technique and Decoding fMRI Patterns. *Current Directions in Psychological Science,* 23**,** 178-183.

PEARSON, J. & BRASCAMP, J. 2008. Sensory memory for ambiguous vision. *Trends Cogn Sci,* 12**,** 334-41.

PEARSON, J., CLIFFORD, C. W. G. & TONG, F. 2008. The functional impact of mental imagery on conscious perception. *Current Biology,* 18**,** 982-986.

PEARSON, J., NASELARIS, T., HOLMES, E. A. & KOSSLYN, S. M. 2015. Mental Imagery: Functional Mechanisms and Clinical Applications. *Trends Cogn Sci,* 19**,** 590-602.

PEARSON, J., RADEMAKER, R. L. & TONG, F. 2011. Evaluating the Mind's Eye: The Metacognition of Visual Imagery. *Psychological Science,* 22**,** 1535-1542.

PELLI, D. G. 1997. The VideoToolbox software for visual psychophysics: transforming numbers into movies. *Spat Vis,* 10**,** 437-42.

RADEMAKER, R. L. & PEARSON, J. 2012. Training Visual Imagery: Improvements of Metacognition, but not Imagery Strength. *Front Psychol,* 3**,** 224.

SACK, A. T., VAN DE VEN, V. G., ETSCHENBERG, S., SCHATZ, D. & LINDEN, D. E. 2005. Enhanced vividness of mental imagery as a trait marker of schizophrenia? *Schizophr Bull,* 31**,** 97-104.

SCHLEGEL, A., KOHLER, P. J., FOGELSON, S. V., ALEXANDER, P., KONUTHULA, D. & TSE, P. U. 2013. Network structure and dynamics of the mental workspace. *Proc Natl Acad Sci U S A,* 110**,** 16277-82.

SCHOLVINCK, M. L., MAIER, A., YE, F. Q., DUYN, J. H. & LEOPOLD, D. A. 2010. Neural basis of global resting-state fMRI activity. *Proc Natl Acad Sci U S A,* 107**,** 10238-43.

SERENO, M. I., DALE, A. M., REPPAS, J. B., KWONG, K. K., BELLIVEAU, J. W., BRADY, T. J., ROSEN, B. R. & TOOTELL, R. B. 1995. Borders of multiple visual areas in humans revealed by functional magnetic resonance imaging. *Science,* 268**,** 889-93.

SHERWOOD, R. & PEARSON, J. 2010. Closing the mind's eye: incoming luminance signals disrupt visual imagery. *PLoS One,* 5**,** e15217.

SHINE, J. M., KEOGH, R., O'CALLAGHAN, C., MULLER, A. J., LEWIS, S. J. & PEARSON, J. 2015. Imagine that: elevated sensory strength of mental imagery in individuals with Parkinson's disease and visual hallucinations. *Proc Biol Sci,* 282**,** 20142047.

SONG, C., SCHWARZKOPF, D. S., KANAI, R. & REES, G. 2011. Reciprocal anatomical relationship between primary sensory and prefrontal cortices in the human brain. *J Neurosci,* 31**,** 9472-80.

STROBACH, T., SOUTSCHEK, A., ANTONENKO, D., FLOEL, A. & SCHUBERT, T. 2015. Modulation of executive control in dual tasks with transcranial direct current stimulation (tDCS). *Neuropsychologia,* 68**,** 8-20.

TERHUNE, D. B., SONG, S. M. & COHEN KADOSH, R. 2015. Transcranial alternating current stimulation reveals atypical 40 Hz phosphene thresholds in synaesthesia. *Cortex,* 63**,** 267-70.

TEUFEL, C., SUBRAMANIAM, N., DOBLER, V., PEREZ, J., FINNEMANN, J., MEHTA, P. R., GOODYER, I. M. & FLETCHER, P. C. 2015. Shift toward prior knowledge confers a perceptual advantage in early psychosis and psychosis-prone healthy individuals. *Proc Natl Acad Sci U S A,* 112**,** 13401-6.

TRAMO, M. J., LOFTUS, W. C., STUKEL, T. A., GREEN, R. L., WEAVER, J. B. & GAZZANIGA, M. S. 1998. Brain size, head size, and intelligence quotient in monozygotic twins. *Neurology,* 50**,** 1246-52.

WANDELL, B. A., DUMOULIN, S. O. & BREWER, A. A. 2007. Visual field maps in human cortex. *Neuron,* 56**,** 366-83.

ZEMAN, A., DEWAR, M. & DELLA SALA, S. 2015. Lives without imagery - Congenital aphantasia. *Cortex,* 73**,** 378-80.

Cortical excitability controls the strength of mental imagery

SUPPLEMENTARY MATERIAL

- **Supplementary Results**
- **Supplementary Figures (9 Figures)**
- **Supplementary Tables (3 Tables)**

Mock difference scores tDCS

1 mA Occipital Stimulation

There was no main effect of tDCS polarity ($F(1,15) = 1.72$, $p = .21$) or block on mock priming (Greenhouse-Geisser correction for violation of sphericity, $F(2,29.99) = 1.58$, $p = .22$), and no interaction between the two (Greenhouse-Geisser correction for violation of sphericity, $F(1.78, 26.62) = .28$, $p = .74$).

1.5 Occipital Stimulation

There was no main effect of tDCS polarity ($F(1,13) = .60$, $p = .45$) or block on mock priming ($F(3,39) = 1.27$, $p = .30$), and no interaction between the two ($F(3,39) = 1.65$, $p = .19$).

1.5 Prefrontal Stimulation

There was no main effect of tDCS polarity ($F(1,16) = .27$ $p = .61$) or block on mock priming ($F(3,48) = .46$, $p = .71$), and no interaction between the two ($F(3,48) = .15$, $p = .93$).

Supplementary Figures

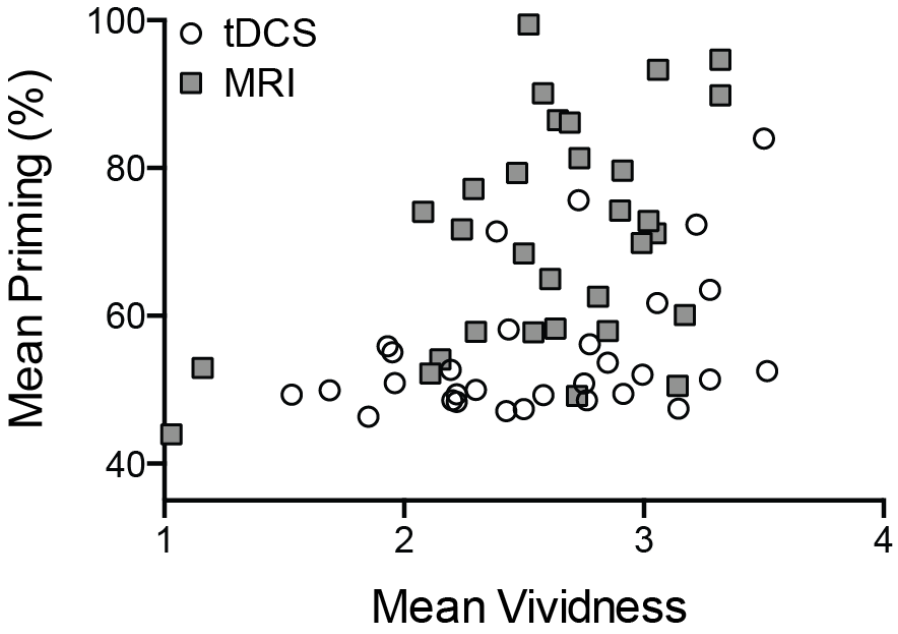

Supplementary figure S1. Data shows the correlation between mean vividness ratings (x-axis) and visual imagery priming (y-axis) for participants from both the MRI and tDCS experiments (tDCS experiment 2 and 3). There was a significant correlation between priming and mean vividness ratings (r_s = .36, p = .005, Spearman's rank-order correlation was used due to a violation of normality). We also computed the correlations between priming and mean vividness separately for the 2 experiments, tDCS and MRI. When this was done correlation between priming and mean vividness was still significant for the tDCS data (r_s = .36, p = .05, Spearman's rank-order correlation was used due to a violation of normality) and was close to significance for the MRI data (r_s = .34, p = .07, Spearman's rank-order correlation was used due to a violation of normality).

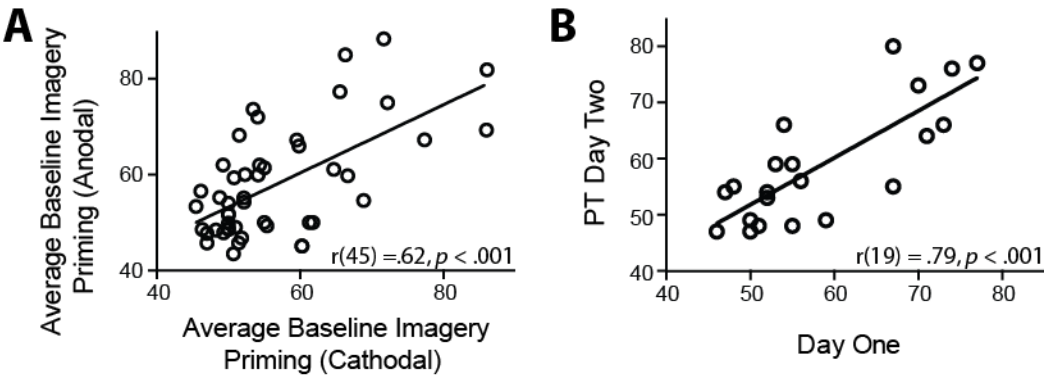

Supplementary figure S2. Re-test reliability for imagery strength (A) and Phosphene Thresholds (B). A. Scatterplot shows participants' imagery strength measured by percent of binocular rivalry displays primed before tDCS stimulation across the two days of testing. Each data point represents one participant, 47 pairs in total. B. Scatterplot shows participants' 60 percent phosphene thresholds (PT) before tDCS stimulation across the two days of testing. Each data point represents one participant, 21 pairs in total.

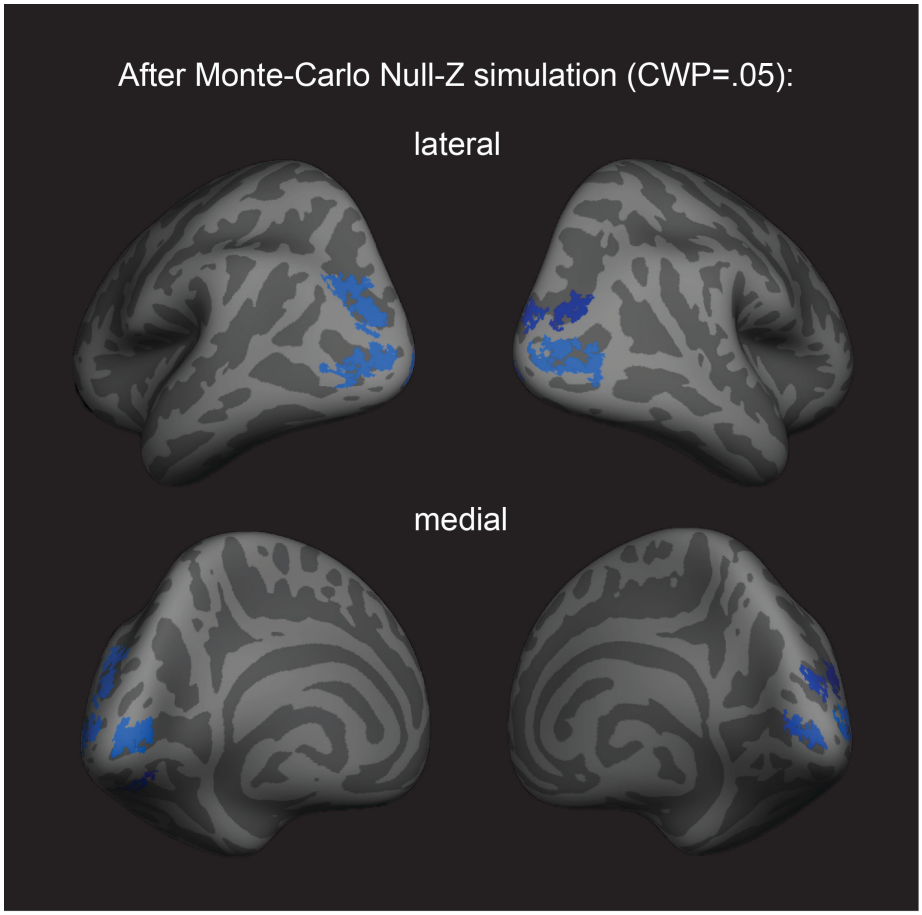

Supplementary figure S3. Surface-based whole brain analysis of the fMRI resting-state data: negative associations with imagery strength. Corrected clusters showing a *negative* association with individual imagery strength at a cluster-wise probability threshold of $P < .05$ (also see **Supplementary Table S1**). In both rows, the two hemispheres are shown from the back. Multiple comparison correction was done using Monte Carlo Null-Z simulation (mc-z). No smoothing of the functional mean intensity data was applied. In line with the correlation analyses using normalised fMRI mean intensity of atlas- and retinotopically defined areas, only fMRI mean intensity clusters in the back of the brain, where early visual and lateral occipital cortex are located, showed negative associations with imagery strength (% primed).

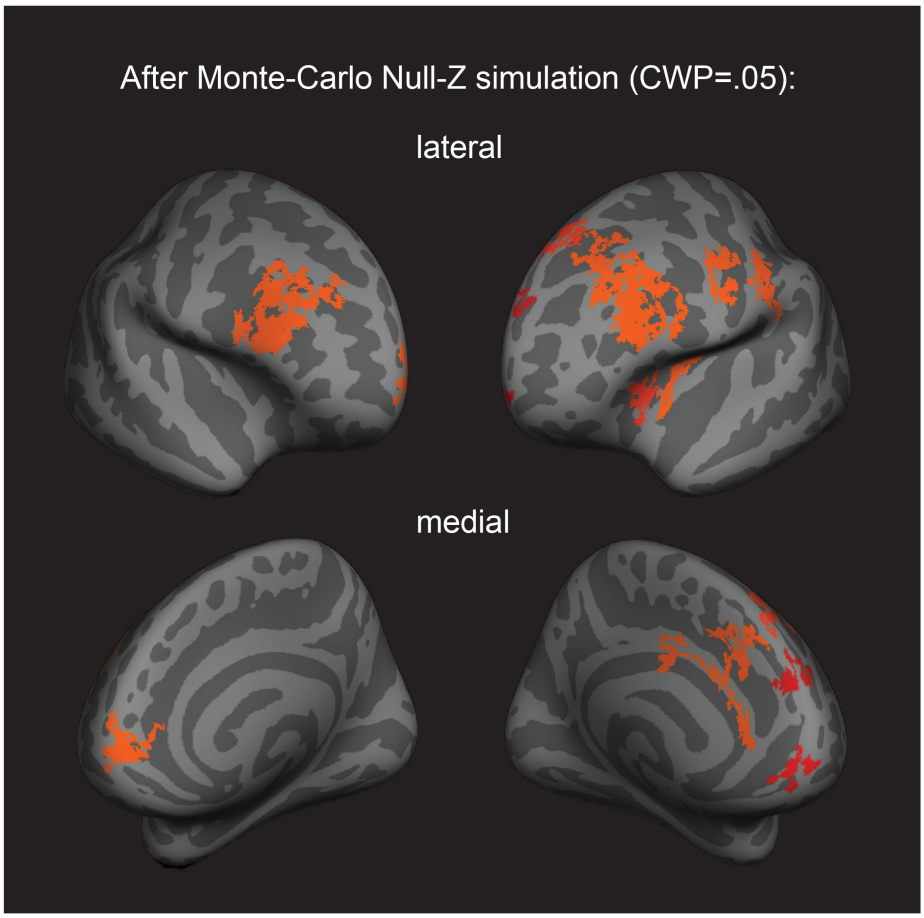

Supplementary figure S4. Surface-based brain analysis of the fMRI resting-state data and imagery: positive associations with imagery strength. Corrected clusters showing a *positive* association with individual imagery strength at a cluster-wise probability threshold of $P < .05$ (also see **Supplementary Table S2**). In both the lateral and medial view, the hemispheres are shown from the front. Multiple comparison correction was done using Monte Carlo Null-Z simulation (mc-z). No smoothing of the functional data was applied. In line with the correlation analyses using normalised fMRI mean intensity of atlas- and retinotopically defined areas, only fMRI mean intensity clusters in frontal areas showed positive associations with imagery strength (% primed).

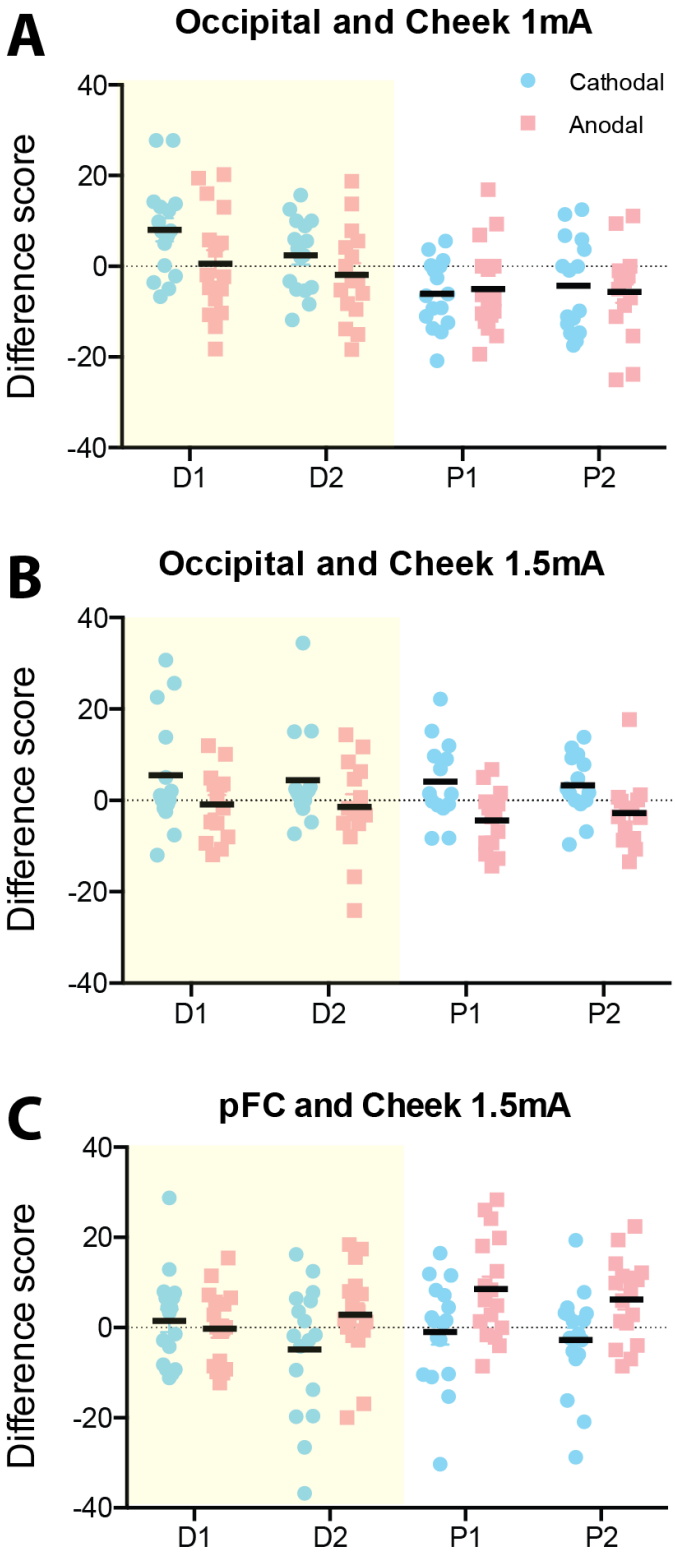

Supplementary figure S5. Spread of individual data points in difference scores for experiment 1 (A), experiment 2 (B) and experiment 3 (C). Blue data points represent individual subjects' cathodal stimulation changes while red data points represent anodal stimulation changes. The figure shows difference scores for each imagery block, two during (D1 and D2, shaded yellow area) and two after tDCS (P1 and P2).

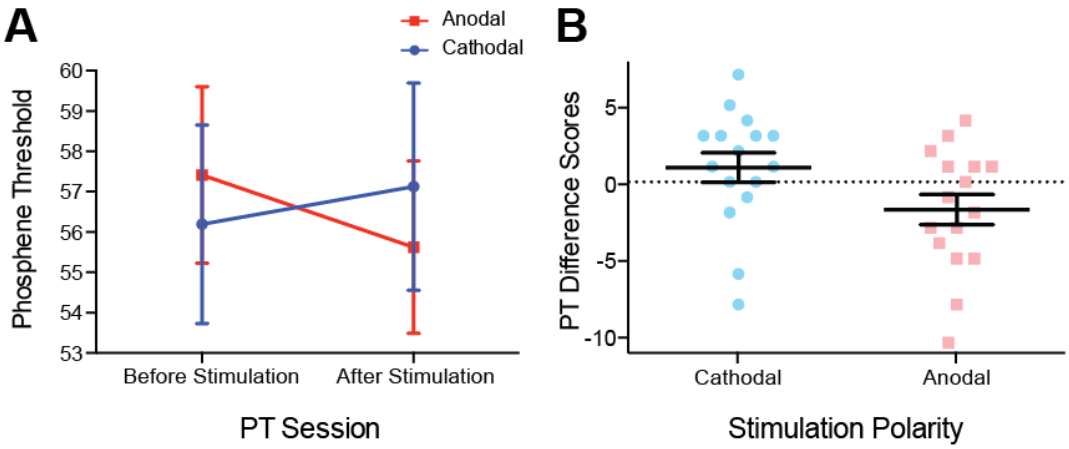

Supplementary figure S6. **tDCS modulation of phosphene thresholds. A.** Data shows phosphene thresholds (PT) before cathodal (left hand side, blue data points) and before anodal (left hand side, red data points) and after cathodal (right hand side, blue data points) and after anodal stimulation (right hand side, red data points). A significant interaction between tDCS polarity and PT session was found ($F(1,15) = 6.03$, $p < .05$). **B.** We then looked at the difference scores for each participant's phosphene thresholds in the cathodal and anodal conditions. This difference score was calculated with the following equation: $PT_{(after\ tDCS)} - PT_{(before\ tDCS)}$. Data shows participants' phosphene threshold differences scores with positive scores indicating that PTs have increased after tDCS (in the cathodal condition, blue bar) while negative scores indicate that PTs have decreased after tDCS (in the anodal condition, red bar). There was a significant difference between the anodal and cathodal conditions with anodal PT changes being significantly lower than cathodal ($t(15) = 2.46$, $p < .05$). All error bars show ±SEMs.

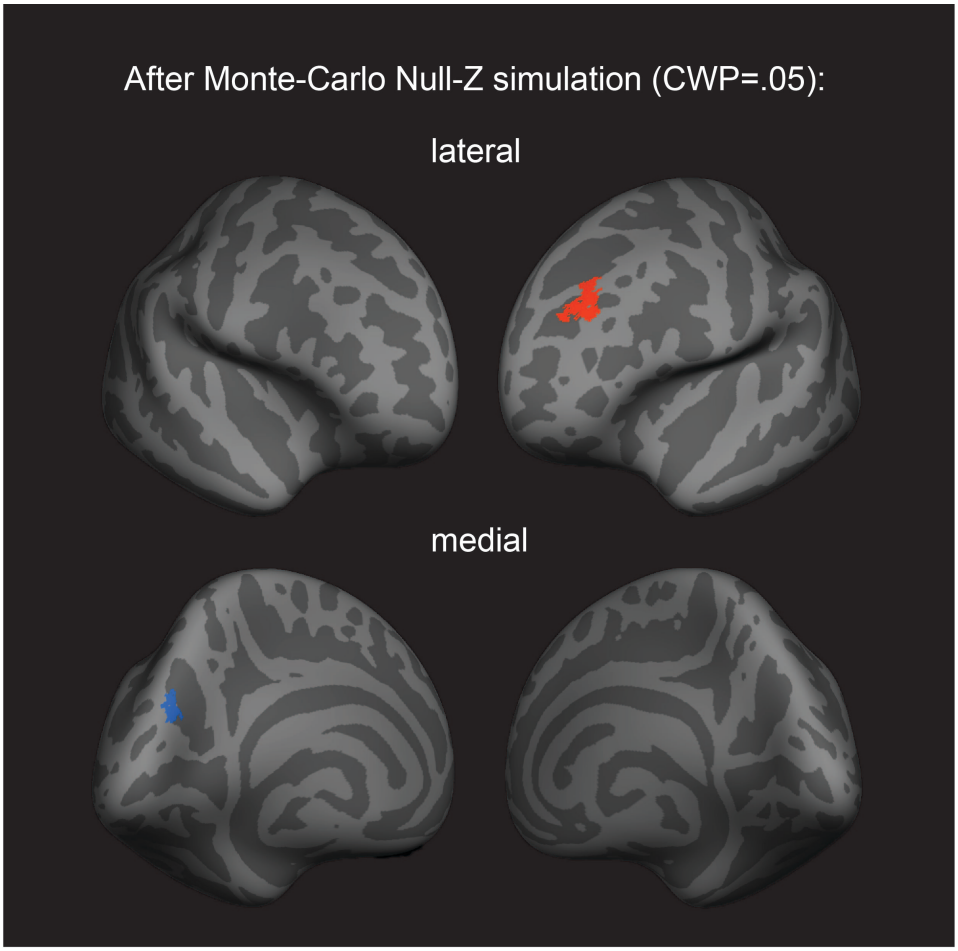

Supplementary figure S7. Surface-based whole brain analysis of the fMRI resting-state data: associations with subjective vividness. Corrected clusters showing associations with individual subjective vividness at a cluster-wise probability threshold of $P < .05$ (see also see **Supplementary Table S3**). The upper row shows a lateral view of the two hemispheres from an anterior perspective, whereas the lower row shows a medial view of them from the back. Multiple comparison correction was done using Monte Carlo Null-Z simulation (mc-z). No smoothing of the functional data was applied. Only two fMRI mean intensity clusters showed associations with subjective vividness that survived the correction for multiple comparisons: One cluster in the left rostralmiddlefrontal cortex showed a positive association (orange), and one smaller cluster in the left cuneus showed a negative association (blue). Note the similarity in the subjective vividness results with the ones in Bergmann et al. (2015), where only a volume cluster in left frontal cortex also showed a positive association with subjective vividness. Apparently, the positive relationship of subjective vividness with the anatomy of left frontal cortex is also reflected in the fMRI mean intensity levels of this region.

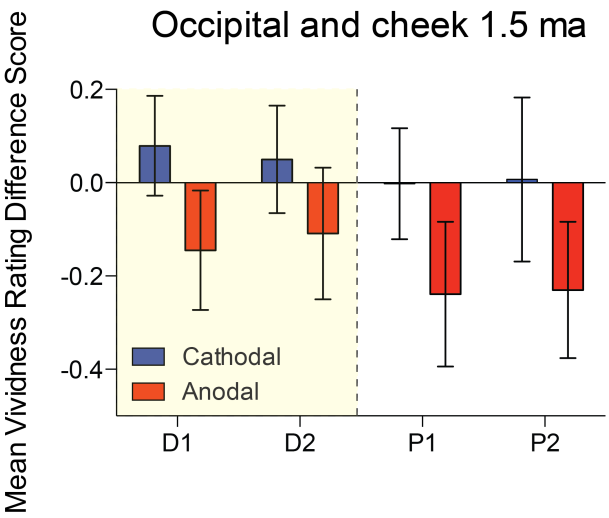

Supplementary figure S8. tDCS of occipital cortex and mean vividness ratings. Vividness ratings were included in this experiment, which allowed us to look at subjective changes in imagery vividness that occur with changes in cortical excitability of the visual cortex. Red bars show the effect of anodal stimulation (increasing excitability) while blue bars show cathodal stimulation (decreasing excitability). All data show means and error bars represent ±SEM's. The data was again analyzed using difference scores calculated by: Block(n) – Average Pre Priming. We found no significant differences in the reported mean vividness of the imagined patterns (main effect of tDCS polarity: $F(1,13) = 2.67$, $p = .13$, main effect of block: $F(3,39) = 1.31$, $p = .29$, interaction: $F(3,39) = .35$, $p = .79$), however in the anodal condition the majority of differences scores are negative indicating less vivid images, see supplementary figure S6.

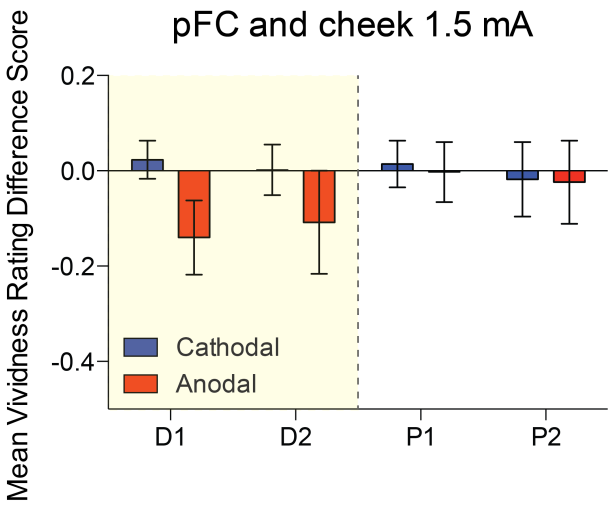

Supplementary figure S9. tDCS of prefrontal cortex and mean vividness ratings. As vividness ratings were included in this experiment, we could also look at the subjective changes in imagery vividness that occur with changes in cortical excitability of the prefrontal cortex. Red bars show the effect of anodal stimulation (increasing excitability) while blue bars show cathodal stimulation (decreasing excitability). All data show means and error bars represent ±SEM's. We again analyzed the data using difference scores calculated by: Block(n) – Average Pre Priming. There were no differences in the mean vividness ratings for either polarity of the tDCS (main effect: $F(1,16) = 1.40$, $p = .25$) or the block (main effect: $F(3,48) = .50$, $p = .68$), and there was no interaction between the two ($F(3,48) = 1.32$, $p = .28$), see supplementary figure S7.

Supplementary Tables

Supplementary Table S1

Surface-based whole brain analysis of the fMRI resting-state data: Corrected clusters showing a significantly *negative* association with individual imagery strength at a cluster-wise probability threshold of $P < .05$ (also see **Supplementary Fig. S1**).

Cluster No.	Maximum voxel-wise significance in cluster	Peak vertex annotation	Size (mm^2)	MNI 305 coordinates of peak vertex			Cluster-wise *P*-value	NVtxs	Laterality	Area label
1	-4.613	11477	552.22	-24.7	-86.6	12.8	0.0002	903	L	lateraloccipital
2	-4.172	97048	535.7	-20.6	-96.9	3.3	0.0002	734	L	lateraloccipital
3	-3.936	130756	534.22	-13.3	-86.4	5.3	0.0002	698	L	pericalcarine
4	-3.053	63050	248.57	-19.5	-80.4	-7.3	0.0024	298	L	lingual
5	-2.848	162967	203.8	-31.3	-59.6	-8.4	0.01276	374	L	fusiform
1	-4.488	69964	301.97	17	-96.6	0.8	0.0004	408	R	pericalcarine
2	-4.021	71800	560.64	27.4	-92.3	1.2	0.0002	785	R	lateraloccipital
3	-3.739	117794	239.69	14.6	-91.3	19	0.0028	301	R	lateraloccipital
4	-2.502	104614	214.22	35.9	-82.5	18.4	0.00519	366	R	inferiorparietal

Note: Correction for multiple comparisons at a cluster-wise probability threshold of $p < .05$ was done using a pre-cached Monte Carlo Null-Z simulation with 10000 iterations. The locations of the clusters strongly overlap with the locations of the atlas- and retinotopically defined areas that showed a negative association with imagery strength. Abbreviations: L = left hemisphere, R = right hemisphere; NVtxs = Number of vertices.

Supplementary Table S2

Surface-based whole brain analysis of the fMRI resting-state data: Corrected clusters showing a significantly *positive* association with individual imagery strength at a cluster-wise probability threshold of $P < .05$ (also see **Supplementary Fig. S2**).

Cluster No.	Maximum voxel-wise significance in cluster	Peak vertex annotation	Size (mm^2)	MNI 305 coordinates of peak vertex			Cluster-wise *P*-value	NVtxs	Laterality	Area label
1	3.775	108491	470.82	-52.7	-21.2	33.4	0.0002	1019	L	postcentral
2	3.749	95009	440.42	-40.1	-13.9	20.6	0.0002	1163	L	insula
3	3.715	121748	1668.23	-43.2	29.7	25.7	0.0002	2992	L	rostralmiddlefrontal
4	3.463	82836	192.99	-8.3	31.5	53.6	0.01514	368	L	superiorfrontal
5	3.26	82794	292.83	-17.5	27.1	50.2	0.0004	462	L	superiorfrontal
6	3.171	119359	377.67	-47.1	-9.1	24.9	0.0002	928	L	postcentral
7	2.908	129777	250.18	-7.3	53.6	-6.2	0.0016	315	L	medialorbitofrontal
8	2.897	34901	238.38	-7.1	56	25.3	0.0026	382	L	superiorfrontal
9	2.848	117187	597.68	-9.9	30	31.1	0.0002	1199	L	superiorfrontal
10	2.180	102903		-35.3	13.6	-4.9	0.0004	747	L	insula
11	1.886	153160		-11.6	49.8	7.8	0.03096	298	L	superiorfrontal
1	4.499	102470	1518.23	44.3	31.2	21.4	0.0002	2730	R	rostralmiddlefrontal
2	3.291	48386	195.37	23	0.5	60	0.01236	435	R	superiorfrontal
3	2.698	51226	417.29	8.3	61.7	-0.8	0.0002	572	R	superiorfrontal
4	2.445	46598	185.98	17.4	-10.8	60.3	0.01851	377	R	precentral

Note: Correction for multiple comparisons at a cluster-wise probability threshold of $p < .05$ was done using a pre-cached Monte Carlo Null-Z simulation with 10000 iterations. The locations of the clusters are strongly overlapping with the locations of the atlas-defined areas that showed a positive association with imagery strength. Abbreviations: L = left hemisphere, R = right hemisphere; NVtxs = Number of vertices.

Supplementary Table S3

Surface-based whole brain analysis of the fMRI resting-state data: Corrected clusters showing significantly positive and negative associations with individual subjective vividness at a cluster-wise probability threshold of $P < .05$ (also see **Supplementary Fig. S3**).

Cluster No.	Maximum voxel-wise significance in cluster	Peak vertex annotation	Size (mm^2)	MNI 305 coordinates of peak vertex			Cluster-wise *P*-value	NVtxs	Laterality	Area label
1	-3.067	21503	185.66	-10.9	-78.5	24.4	0.02405	239	L	cuneus
2	2.526	42871	290.45	-31.3	32	33.7	0.0004	480	L	rostralmiddlefrontal

Note: Correction for multiple comparisons at a cluster-wise probability threshold of $p < .05$ was done using a pre-cached Monte Carlo Null-Z simulation with 10000 iterations. Abbreviations: L = left hemisphere, R = right hemisphere; NVtxs = Number of vertices.